Solid-State and Vacuum Thermionic Energy Conversion

A. Shakouri, Z. Bian, R. Singh, Y. Zhang, D. Vashaee, T. E. Humphrey and H. Schmidt
Baskin School of Engineering
University of California at Santa Cruz

J. M. Zide, G. Zeng, J-H. Bahk, A. C. Gossard and J. E. Bowers
Materials Department, Electrical and Computer Engineering
University of California at Santa Barbara

V. Rawat and T. D. Sands
Materials Engineering, Electrical and Computer Engineering
Purdue University

W. Kim, S. Singer and A. Majumdar
Mechanical Engineering Department
University of California at Berkeley

P. M. Mayer and R. J. Ram
Research Laboratory of Electronics
Massachusetts Institute of Technology

K. J. Russel and V. Narayanamurti
Division of Engineering and Applied Sciences
Harvard University

F.A.M. Koeck, X. Li, J.-S. Park, J.R. Smith, G.L. Bilbro, R.F. Davis, Z. Sitar, R.J. Nemanich
Departments of Physics, Materials Science and Engineering and Electrical and Computer Eng.
North Carolina State University

ABSTRACT
A brief overview of the research activities at the Thermionic Energy Conversion (TEC) Center is given. The goal is to achieve direct thermal to electric energy conversion with >20% efficiency and >1W/cm^2 power density at a hot side temperature of 300-650C. Thermionic emission in both vacuum and solid-state devices is investigated. In the case of solid-state devices, hot electron filtering using heterostructure barriers is used to increase the thermoelectric power factor. In order to study electron transport above the barriers and lateral momentum conservation in thermionic emission process, the current-voltage characteristic of ballistic transistor structures is investigated. Embedded ErAs nanoparticles and metal/semiconductor multilayers are used to reduce the lattice thermal conductivity. Cross-plane thermoelectric properties and the effective ZT of the thin film are analyzed using the transient Harman technique. Integrated circuit fabrication techniques are used to transfer the n- and p-type thin films on AlN substrates and make power generation modules with hundreds of thin film elements. For vacuum devices, nitrogen-doped diamond and carbon nanotubes are studied for emitters. Sb-doped highly oriented diamond and low electron affinity AlGaN are investigated for collectors. Work functions below 1.6eV and vacuum thermionic power generation at temperatures below 700C have been demonstrated.

INTRODUCTION

Direct thermal to electrical energy conversion systems that could operate at lower temperatures (300-650C) with high efficiencies (>15-20%) provide an attractive compact alternative to internal combustion engines for many applications in the W-MW range. They will also expand the possibilities for waste heat recovery applications. The Thermionic Energy Conversion Center's goal is to design, fabricate, and characterize direct energy conversion systems that meet the above requirements. The core of the solution is an integrated approach to engineer electrical and thermal properties of nanostructured materials and devices and fabricate more efficient solid-state and vacuum-based thermionic energy conversion systems. Solid-state material design is focused on increasing the efficiency of heterostructure thermionic power generators using embedded nanoparticles and metal/semiconductor superlattices. Vacuum effort focuses on the development of thermionic energy conversion based on thermionic-field emission from nanostructured carbon surfaces and low work function n-type wide band gap semiconductor collectors. Measurements of electrical, optical and thermal transport at both the device and nanostructure level are used to verify model predictions and thereby lay the foundation for improved device and materials design. Finally, various components will be integrated and packaged for systems demonstration. Fig. 1 displays a chart of the research groups participating in the Thermionic Energy Conversion Center.
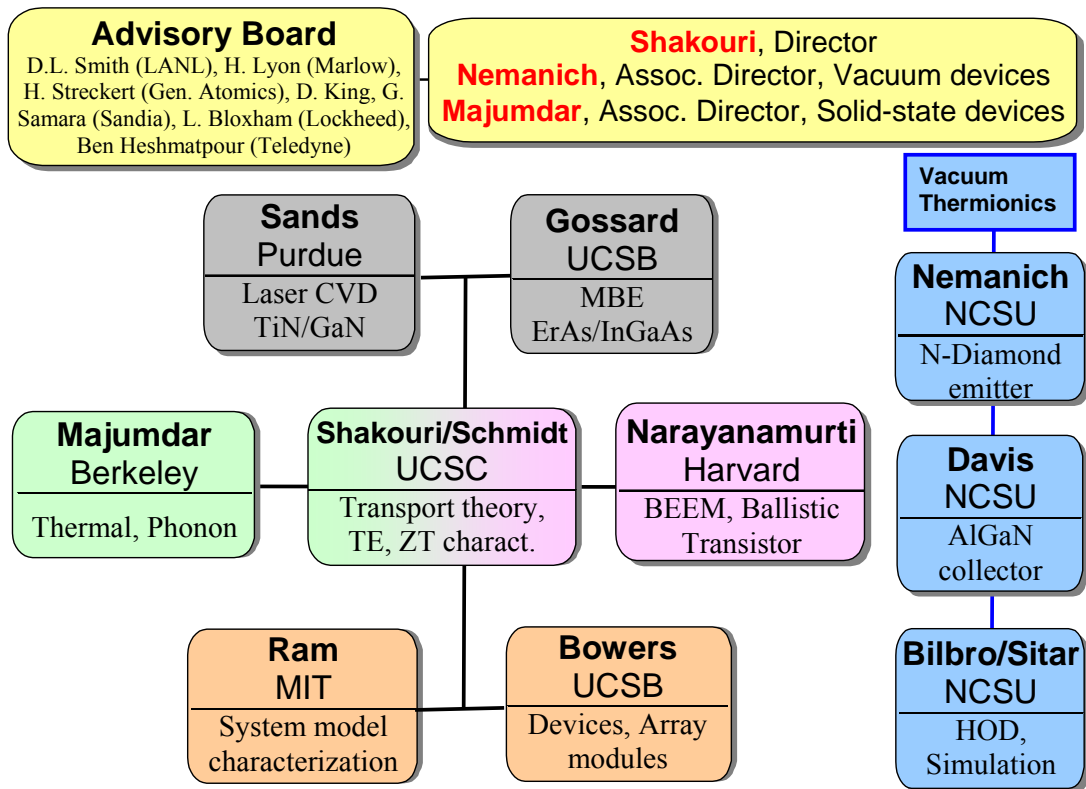
Thermionic Energy Conversion Center

Fig. 1 Thermionic Energy Conversion Center and the efforts on solid-state and vacuum devices.

SOLID-STATE DEVICES
Theoretical Analysis
The motivation to work on metal-based superlattices and embedded nanoparticles was based on the theoretical calculation of Vashaee and Shakouri [1] who predicted ZT>5 for optimized structures even with a lattice contribution to thermal conductivity on the order of 1W/mK. The main idea is that in a thermoelectric energy conversion device work is extracted from the random thermal motion of electrons, so in principle we would like to have as many electrons as possible in the material. However, highly degenerate semiconductors and metals are not good bulk thermoelectric materials due to their low Seebeck coefficient. In reference [2], we analyzed the trade off between electrical conductivity and the Seebeck coefficient and explained that highly degenerate semiconductors and metallic structures can have high thermoelectric power factors (Seebeck coefficient square times electrical conductivity) if there is an appropriate hot electron filter (potential barrier) that selectively scatters cold electrons. Here, in the near linear transport regime, hot electrons denote carriers that contribute to electrical conduction with energies higher than the Fermi level and cold electrons have energies lower than the Fermi level. This nomenclature is different from device physics where hot carriers are typically non-equilibrium populations which can be built up under high electric fields.

The concept of hot electron filters using heterostructure barriers was first introduced in Ref. [3]. However in the case of single barrier structures under high biases (non-linear transport regime), the energy conversion efficiency is not higher than the bulk case, but very high power densities can be achieved. Mahan et al. first suggested that multi barrier thermionic structures could have high efficiencies [4], however later analysis showed that the power factor of small barrier superlattices is indeed not very different from the bulk values. The advantage of multibarrier structures was claimed to be in lowering of the lattice thermal conductivity [5]. Highly efficient tall barrier metallic superlattices were first suggested in 1998 [6], however detailed modeling of electron transport in these structures revealed the importance of lateral momentum non-conservation [7]. The basic idea is that planar superlattices are momentum filters and not energy filters. Only hot electrons with a large enough kinetic energy in the direction perpendicular to barriers are transmitted, while lots of other hot electrons are blocked. In order to achieve non-conversation of lateral momentum in the thermionic emission process one can break the translation invariance in the plane of superlattices or use 3D potential barriers [8]. Hence the emphasis of the solid-state activities at the TEC Center is to use embedded nanoparticles and non-planar barriers.

In order to verify our theoretical modeling of electron transport, which was the basis for the design of novel power generation materials, we first applied the theory to predict variable temperature current-voltage characteristics of multi quantum well structures used ,e.g., infrared detector applications [9].Vast literature of experimental results for dark current in III-V superlattices is available. At low temperatures, current in the device is extremely sensitive to temperature; it can easily change by 4-8 orders of magnitude with a slight increase of 50-100K in temperature. Our theoretical curves matched the experimental results that assume lateral momentum in the planar superlattices is

conserved [10]. In brief, electron transport is modeled by a bulk-type linear Boltzmann equation with a correction due to the quantum mechanical transmission above and below the barrier. Since the optimum Fermi energy is close to barrier height and 3D states contribute significantly to electronic transport, it is also important to consider both 2D states in the wells and 3D states in the barrier.. We further verified the theory by analyzing the cross-plane Seebeck coefficient in short period InGaAs/InAlAs superlattices (lattice matched in InP) [11]. In these structures, as the doping is increased, the Seebeck coefficient shows a non-monotonic behavior. This is quite different from bulk materials and it is due to the formation of superlattice minibands. Theoretical curves matched well the experimental results for the 4 samples with different dopings in a wide temperature range.

Bian and Shakouri have recently developed a Monte Carlo program in order to investigate how non-planar barriers can affect electron transport and evaluate non-conservation of lateral momentum [12]. This program allows us to calculate the average number of electrons transmitted above an arbitrary shaped two-dimensional potential barrier. The average transport energy of the transmitted electrons, i.e., the Seebeck coefficient, can also be calculated. Preliminary results show that non-planar barriers have indeed larger thermoelectric power factors compared to planar ones. Another important issue in the superlattice structures is that the electron wave interference affects both the electronic density of states and the electron transmission probability. While one can use the miniband density-of-states in the limit of very short superlattice periods, one usually considers 2D states in the limit of isolated quantum wells. For thermionic power generation, we would like to have barrier thickness to be on the order of the electron mean-free-path. In this important intermediate transport regime, it is not easy to calculate the density-of-states, especially for the 3D states in the barrier. Humphrey and Shakouri are using a probabilistic approach to calculate the transport properties that take into account electron interference effects within the electron scattering length [13]. We hope that this will allow us to optimize the superlattice period for maximum efficiency. This could also be generalized to model electron transport in 3D embedded nanoparticle structures.

The theoretical analysis presented earlier showed the potential of metal-based hot-electron filters. Many metals can be grown epitaxially on top of semiconductors, however growth of high quality semiconductors on top of metals is difficult. There are not many candidate systems for high quality, high-electron-mobility, metal/semiconductor, composites. In the MURI TEC Center, we concentrate on two material systems: the first one is ErAs:InGaAlAs and the second one is TiN/GaN multilayers.

InGaAs with embedded semimetallic ErAs nanoparticles
ErAs is a rocksalt semimetal which forms into epitaxial nanometer-sized particles on a III-V semiconductor surface. Overgrowth is nucleated on the exposed semiconductor surface between the particles and is essentially defect-free. The properties of the resulting nanocomposite are dependent on the composition of the host semiconductor and on particle morphology, which can be controlled during growth. For thermoelectric applications, we concentrated on the incorporation of ErAs into various compositions of

InGaAlAs (lattice matched to InP). The particles pin the Fermi level at an energy that is dependent both on the particle size and the composition of the semiconductor. For example, the Fermi level of InGaAs is pinned within the conduction band, increasing the free electron concentration and thus the electrical conductivity. We first focused on developing structures which consisted of superlattices of ErAs islands in an InGaAs matrix, which was lattice matched to an InP substrate (see . 2a). To maintain a constant ErAs concentration our initial samples consisted of ErAs depositions ranging from 0.05 monolayers/period to 0.4 monolayers/period, with the superlattice period varying from 5 nm to 40 nm. While InGaAs is not a good thermoelectric materials to start with (room temperature ZT ~ 0.05), the incorporation of ErAs reduced the thermal conductivity of the material by approximately a factor of 2 (i.e., total thermal conductivity ~4W/mK) [14]. At the same time, in-plane measurements of the Hall effect showed an increased carrier concentration for smaller particles and a high-quality material with mobilities of 2000-4000 cm^2/Vs at 300K [15]. We then concentrated on the growth of co-deposited (randomly distributed) ErAs:InGaAs, which has the advantage of growing much faster than superlattice structures because it does not require growth interrupts (see Fig. 2b). This allows us to grow much thicker structures with greater stability. Our initial efforts focused on 0.3% ErAs, which is the same concentration as the initial superlattice samples. The Hall effect and Seebeck measurements have shown that these materials are electrically very similar to the superlattice materials with a thermoelectric power factor (Seebeck square times electrical conductivity) similar to bulk InGaAs [15]. On the other hand, the thermal conductivity was reduced by 25% compared to the ErAs/InGaAs superlattice material [14]. The significant reduction compared to bulk alloy material (a factor of 2.5-3) is due to the increased scattering of mid- to long- wavelength phonons by embedded nanoparticles. This makes this system one of the only materials in which thermal conductivity is reduced below the so-called "alloy limit" without creating defects that lower electron mobility and electrical conductivity. We have recently developed a detailed model for phonon transport in these structures, and the simulated lattice thermal conductivity matches well the experimental result over a wide temperature range [16].
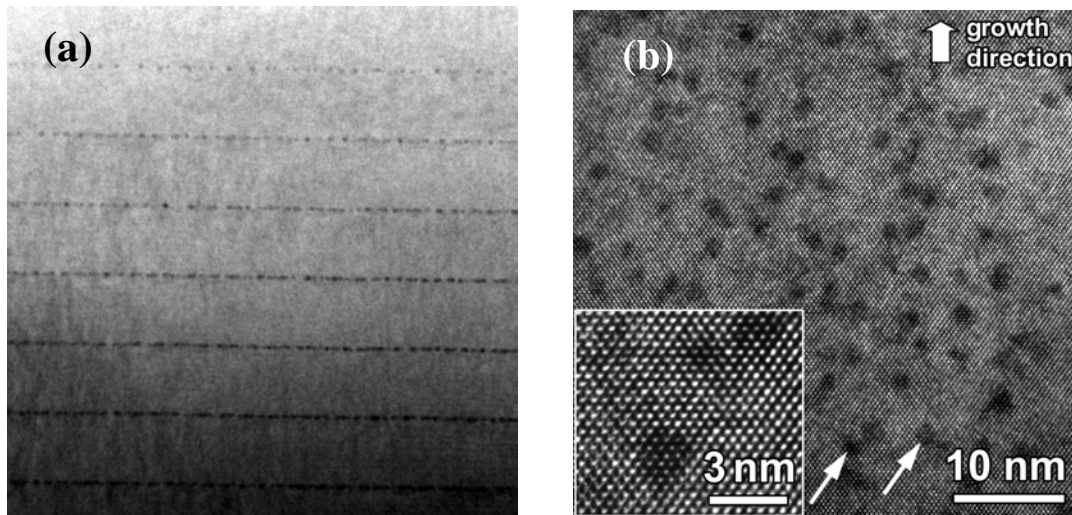

Fig. 2 (a) Tranmission electron micrograph of ErAs/InGaAs superlattices (in this picture the average ErAs composition is reduced from 0.4 monolayers to 0.05 monolayer from the bottom to top of the graph). **(b)** InGaAs matrix with randomly-distributed ErAs nanoparticles.

In order to increase the number of carriers participating in transport and improve the thermoelectric power factor, we studied n-type ErAs:InGaAs structures with InGaAlAs barriers for electron filtering. These barriers actually consist of a short-period superlattice or "digital alloy" of InGaAs and InAlAs. By carefully choosing the composition of the InGaAlAs/InGaAs superlattices, we can create electron filtering barriers to improve the thermoelectric power factor $S^2\sigma$ at a given temperature. The cross-plane thermoelectric transport properties were measured using mesa structures with integrated thin film heaters which are described in following sections. Experimental results confirmed the increase in the cross-plane Seebeck coefficient and power factor [17,18]. Now our emphasis is to do a similar optimization for p-type material, and to increase the ZT even further by a using different size distribution of ErAs nanoparticles, which can reduce the lattice contribution to thermal conductivity.

TiN/GaN multilayers and superlattices
The TiN/GaN material system is investigated for its potential in solid-state thermionic energy conversion at the higher end of the operating temperature. This material system has high melting points (e.g., 3290ºC for TiN), negligible sublimation, low homologous epitaxial growth temperatures (~0.2-0.3), and excellent corrosion resistance and mechanical hardness. Epitaxial stabilization of the high-pressure rocksalt phase of AlN (an insulator) grown on rocksalt TiN and VN has been demonstrated previously studying studies of nitride multilayers for hard wear-resistant coatings (e.g., see ref. [19]). By analogy, we thought that it may be possible to achieve epitaxial stabilization of rocksalt GaN (believed to be a semiconductor with a 1.7 eV bandgap [20]) on a metallic rocksalt substrate. TiN was chosen for the initial studies because it is the best understood of the metallic nitrides. Upon demonstration of coherent epitaxy in the TiN/GaN system, the material properties could be further optimized by e.g. using InN-GaN alloys to tune the barrier height and suppress the thermal conductivity, and/or investigating higher atomic mass metallic nitride alloys. Initial study showed that indeed growth of fiber-textured (111)TiN/(0001) wurtzite GaN multilayers on (0001) sapphire and (100) MgO are possible (see Fig. 3 [21]). From preliminary transmission electron and x-ray diffraction data, it seems as there are two regimes: pure rocksalt TiN/GaN superlattices at shorter periods and rocksalt-TiN/wurtzite-GaN multilayers at longer periods (>7nm). The thermal conductivities of TiN/GaN multilayers on sapphire substrate (with equal layer thicknesses in the range of 1.8-4nm) were measured using 3ω and time-domain thermoreflectance (in collaboration with Prof. D. Cahill at UIUC) and values in the range of 3.6-8.0W/mK were obtained. Low thermal
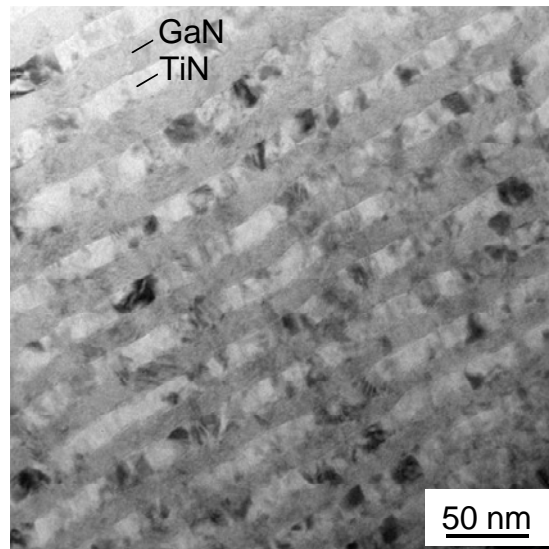

Fig. 3 TEM image of TiN/GaN multilayer grown on (100)MgO. The TiN layers are 15 nm thick. The GaN layer thickness increases from lower right to upper left.

conductivity for such a light-element compounds shows the important contribution of the interface thermal resistances. We are currently investigating the growth of multilayers and superlattices with thicknesses of several microns for device fabrication and also optimizing the superlattice period and barrier height for highest Seebeck coefficient and thermoelectric power factor.

Ballistic transistor structures

It is difficult to extract all the physics of electron transport from a two-terminal current-voltage measurement of a device. Three-terminal ballistic transistor structures allow us to measure the electron mean-free-path and the energy-resolved electron transport. The basic idea is shown in Fig. 4. There is a thin $Al_2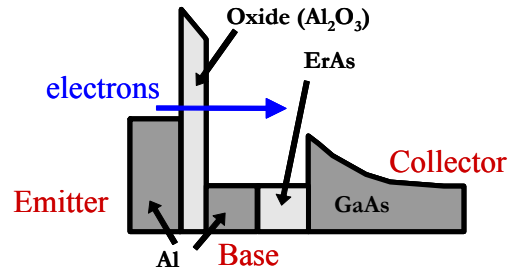O_3$ tunnel junction between the emitter and the base Al layers. Under an applied bias, electrons are injected into the base layer. Since tunneling current is an exponential function

Fig. 4 Ballistic transistor structure used to measure the energy-resolved electron transport at ErAs/GaAs interface.

of the barrier height, most of the injected electrons are monoenergetic, with energies close to the Fermi level of the metal emitter. Since the base layer is very thin, smaller than the electron scattering length, most of the electrons do not thermalize in this layer; rather, they enter the collector layer and they contribute to the collector current. One can show that the second derivative of the collector current with respect to emitter-base voltage is proportional to the electron transmission probability through the base/collector structure. This value is typically used to measure the band offset between two materials, but a careful analysis of the shape of the curve can also provide information about lateral momentum conservation during a thermionic emission process when electrons move between base and collector layers [22]. Measurements for ErAs/GaAs heterostructures agree well with the theoretical calculations, assuming 100% randomization of electrons lateral momentum (i.e. non-conserved case). This measurement was done with a planar device structure with a single layer of ErAs deposited on top of GaAs. We are planning to do similar measurements for InGaAs/InGaAlAs heterostructures both with and without embedded ErAs nanoparticles and investigate their role in lateral momentum scattering. It is possible to do similar three-terminal measurements with even individual nanoparticles with the use of a scanning tunneling microscope tip near the surface, a configuration that is called ballistic electron emission microscopy (BEEM) [23]. Indeed, BEEM has been used to probe the energy states of individual embedded quantum dots [24].

Thin film material properties characterization

We used 50-100µm diameter mesa structures and integrated thin film heater/sensors on top of the superlattice layer to characterize the cross-plane Seebeck coefficient in a wide range of temperatures (see Fig. 5) [25,26]. The difficulty of characterizing the Seebeck coefficient of a superlattice material lies in simultaneously measuring the voltage and temperature drops to within a few microns on both sides of a thin film. In the above measurement, there could be a significant portion of the temperature drop across the

substrate. In order to calculate the substrate contribution, similar thin film heaters were fabricated on a sample where the superlattice was etched away. By using differential measurements, the contribution of the superlattice could be accurately deduced [27].
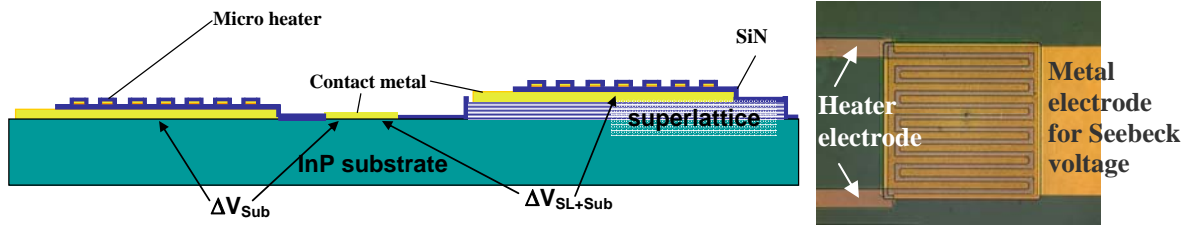

Fig. 5 Integrated thin film heater structure used to measure the cross-plane Seebeck coefficient. Electrical contact layer on top of the superlattice and on the substrate allow measuring the thermoelectric voltage. The thin film resistor acts both as a source of the heat and as a temperature sensor. Differential measurements on top of the superlattice and on the substrate are needed in order to extract both the thin film cross-plane Seebeck coefficient and also the substrate Seebeck.

Transient ZT measurement

In order to extract the intrinsic cross-plane *ZT* of the superlattice by eliminating the effects of the substrate and any parasitics, the bipolar transient Harman technique was used to measure the device *ZT* of samples with different superlattice thicknesses [28]. High-speed packaging is needed to reduce signal ringing due to any electrical impedance mismatch. We achieved a short time resolution of roughly 100ns in a transient Seebeck voltage measurement [29]. Detailed 3D thermal simulations showed the importance of heat transfer along the leads connected to the top of the superlattice [30]. Due to the large device area, compared to the superlattice thickness, heat transfer along the probes can create a non-uniform temperature distribution on top of the superlattice; moreover, a significant fraction of the Peltier heating could be transported through the leads. Both of these effects will influence the transient Harman technique and will lead to wrong ZT values. Once the device and lead geometry were optimized, accurate ZT measurements could be achieved. The measured intrinsic cross-plane *ZT* of the ErAs:InGaAs/InGaAlAs superlattice structure with a doping of 1×10^{19} cm^{-3} is 0.13 at room temperature [29]. This value agrees with both calculations based on the Boltzmann transport equation and direct measurements of specific film properties. Theoretical calculations predict that the cross-plane *ZT* of this superlattice will be greater than 1 at temperatures greater than 700K [18]. Our current emphasis is to use femtosecond laser pump-probe technique to measure the thermal diffusivity and electron mobility perpendicular to the thin film layer.

System requirements

In order to reach the goal of our center and demonstrate direct thermal to electric energy conversion with efficiencies higher than 20%, an average ZT of the material >1.5 through the temperature range of 300-950K is necessary. This can be achieved by grading the material (e.g. changing the superlattice period, barrier height, doping, etc.) and optimizing the properties to maximize the performance at each local temperature. Power generation density is inversely proportional to the thermoelectric leg length, and a goal of 1W/cm^2 will require legs shorter than 1cm. With growth techniques such as molecular beam epitaxy and laser assisted CVD, it is extremely hard to grow thick layers. Thick
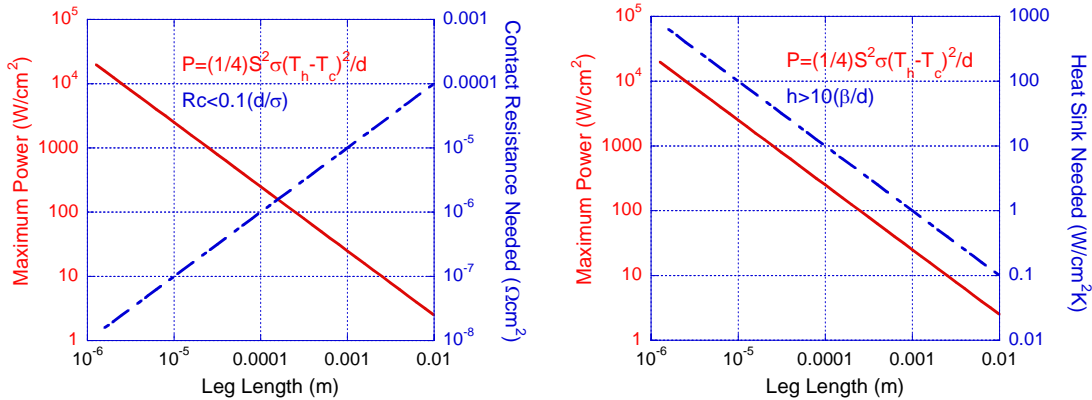
Fig. 6 Power density of an ideal thermoelectric generator as a function of leg length. The minimum required metal-semiconductor contact resistance, as well as the heat sink requirement are also given.

layers also require a lot of nanostructured material and it is quite expensive. If thinner material is used, higher power densities can be achieved. However parasitic loss mechanisms could start to dominate. The key factors are metal/semiconductor electrical contact resistance and the finite thermal resistance of the heat sink. Assuming generic material parameters: Seebeck coefficient $S=200\mu V/K$, electrical conductivity $\sigma=1000/\Omega cm$, thermal conductivity $\beta=1W/mK$, a hot side temperature of $T_h= 900K$ and cold side temperature of $T_c=400K$, Fig. 6 shows the generated power versus device length d. This figure also shows the minimum contact resistance R_c and the minimum heat transfer coefficient h_c needed so that the parasitics do not dominate the generator performance (i.e. their contribution is 10% or less). One can see that with 10 microns thick devices, a contact resistance less than 10^{-7} Ωcm^2 is needed. This is quite possible. On the other hand, a 10 micron device will need a heat sink with a heat transfer coefficient of $100W/cm^2K$, if not; the performance will be significantly degraded. This requirement is orders of magnitude higher than the best sink demonstrated to date, so heat sinking is a quite important limiting factor. On the other hand, the goal of our program is not to generate more than $1000W/cm^2$ that an ideal 10 microns thick device could achieve! One can reduce the heat sink requirement by only covering a fraction F of the hot and cold surfaces with the thermoelectric material (see Fig. 7). This will limit the flow of the heat to the hot side. Of course the fractional coverage only works when there is good heat spreading at the hot and cold surfaces, so F can not be very low. With 1% coverage, one can produce 10's W/cm^2 with a heat sink requirement of $1W/cm^2K$.

Assuming that the hot and cold side temperatures of the thermoelectric leg are constant, it is instructive to note that the expression of the conventional power generation density depends only on the thermoelectric power factor, and it increases as the thickness is reduced: $P=(1/4) S^2\sigma(T_h-T_c)^2/d$.
On the other hand, if we assume a heat sink with finite thermal resistance, the expression of power generation density will also depend on material's thermal conductivity and there

is an optimum thickness that gives the maximum power. In the limit of *small temperature gradients*, (i.e. $(T_h-T_c)/4 << T_c$) the following analytical expressions could be derived:

$$d_{optimum} \cong \frac{\beta\left(1+\frac{1}{2}Z\overline{T}\right)F}{h_c}$$

$$P_{max} \cong \frac{1}{16}\frac{h_c}{\overline{T}}\frac{Z\overline{T}}{1+\frac{1}{2}Z\overline{T}}\left(T_{hot}-T_{fluid}\right)^2$$

where $\overline{T}=(T_h+T_c)/2$. One can see that the optimum thickness is inversely proportional to the heat transfer coefficient, and it can be reduced by fractional coverage of the surfaces. The maximum power generation density is directly proportional to the heat transfer coefficient, it is a function of ZT of the material, but it saturates at high ZT values, and more importantly, the maximum power generation density is independent of *F* as long as heat spreading thermal resistance can be neglected. The above expressions are not a good approximation under large temperature gradients and for a more accurate analysis a 2nd degree equation based on the heat balance in the device should be solved. This makes the solution not very intuitive. However the main conclusions regarding an optimum module thickness, the effect of fractional coverage and the importance of the heat sink remain valid. In a situation when heat transfer from the hot source is also a limiting factor, one can show that the above expressions for optimum thickness and maximum power can be generalized by replacing h_c by $h_c h_h/(h_c+h_h)$ where h_h is the heat transfer coefficient with the hot source. It is interesting to note that when only a fraction of the cold surface is covered by the thermoelectric material and the metal interconnects, one could use the vacant areas and incorporate thermophotovoltaic (TPV) cells that convert the infrared radiation from the hot surface and generate additional electric power.
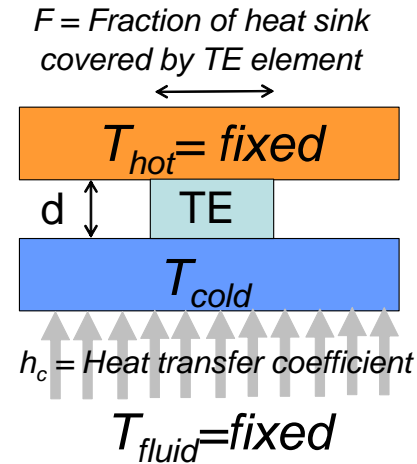

Fig. 7 Thermoelectric power generator where only a fraction of the hot and cold surfaces are covered by the TE element. The cold surface is in contact with non-ideal hat sink.

Module fabrication and system characterization
In order to test the inherent energy conversion efficiency of the material, a test setup has been developed to apply a large temperature difference to a single element and measure the resulting power in an optimum load for power generation. Since the resistance of a single thin film element is very small (mΩ), a special high power MOSFET was used as the tunable resistive load [31]. Heat is applied to the superlattice side of the element with a heater buried in a copper block, and removed from the substrate side of the sample using a cold plate. Between the heat source and sink, the sample is held between two electrically isolated copper blocks. The hot and cold sides of the element are monitored using thermocouples spaced 1 mm from the block surface facing the elements. Experimental results showed that a 5 micron thick n-ErAs:InGaAs/InGaAlAs superlattice on top of 200 micron thick InP substrate with an area of $1\times1mm^2$ could deliver more than

5W/cm^2 under a temperature difference of 300C [32]. We are currently working on a vacuum set up which will allow us to do efficiency measurements accurately.

For the fabrication of multi element thin film power generation module, we chose a wafer scale approach based on IC processing. The first module was based on 5 micron thick n- and p-type ErAs:InGaAs/InGaAlAs superlattices grown on InP substrate [33]. Mesas 7 μm high and 200×200 μm^2 in area were formed by dry etching the InP substrate, and contact and bonding metal layers were deposited on top of these elements using electron beam evaporation. Low contact resistance at the metal/semiconductor interface is a key factor to the thin film generator performance. Ni/GeAu metallization was used to make ohmic contact to the superlattice elements. The sample was annealed at 400 °C for 5 seconds. Specific contact resistivity on the order of 10^{-7} Ω·cm^2 was measured from room temperature up to 250 °C. The array generator was formed via flip-chip bonding: A 200 element n-ErAs:InGaAs/InGaAlAs element array and a 200 element p-ErAs:InGaAs/InGaAlAs are bonded to 650 μm thick upper and lower AlN plates respectively. The InP substrates were removed by wet etching to form n and p thin film element arrays, and these n and p arrays were bonded together to form the 400 element array generator shown in Fig. 8. First trials produced 0.6 mW of output power at a ΔT=30C on an external load resistor of 100Ω. Detailed characterization revealed that most of the temperature drop happens across the AlN plates and that the p-type material is not optimized. We are currently concentrating to further reduce the parasitic heat losses and optimize the superlattice structure which should improve the module performance significantly.
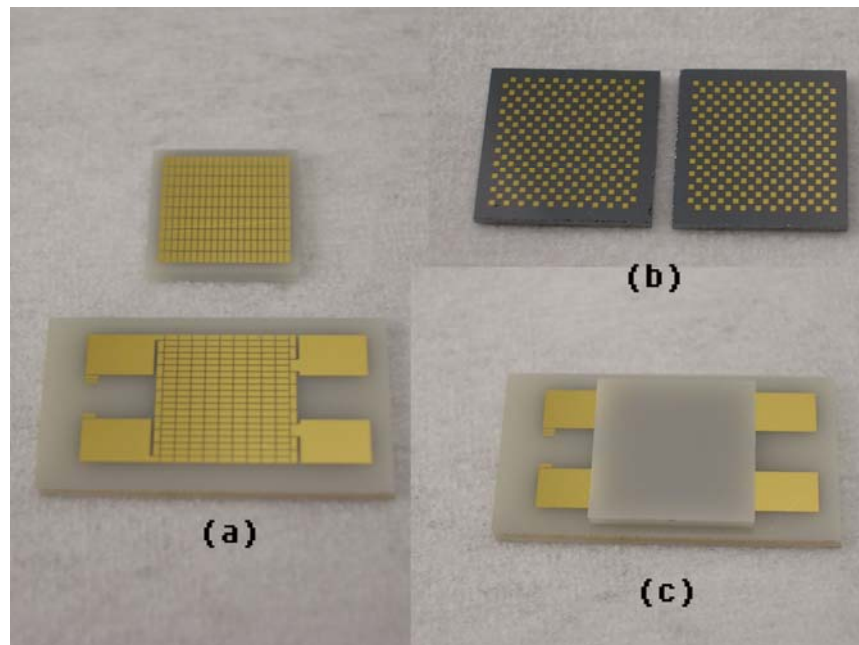

Fig. 8 Photos of AlN plates, Each ErAs:InGaAs/InGaAlAs element array and packaged generator: (a) upper and lower 650 μm thick AlN package plates, (b) of n and p ErAs:InGaAs/InGaAlAs superlattice element arrays, and (c) 400 element thin film ErAs:InGaAs/InGaAlAs superlattice generator. The module size is on the order of 1x1cm^2.

VACUUM THERMIONIC ENERGY CONVERSION

Energy conversion based on vacuum thermionic emission has been explored for many years and prototype systems have been developed and tested. The operation is based on the thermionic emission of electrons from a hot surface and the collection of the electrons at a cooler collector. The emitter and collector are separated by a small vacuum gap. Since the thermionic emission involves hot electrons, these electrons carry excess energy which can be converted into electrical power. The operation may be described in a motive diagram as shown in Fig. 9. In this diagram the operation is in a regime where space charge effects can be neglected.
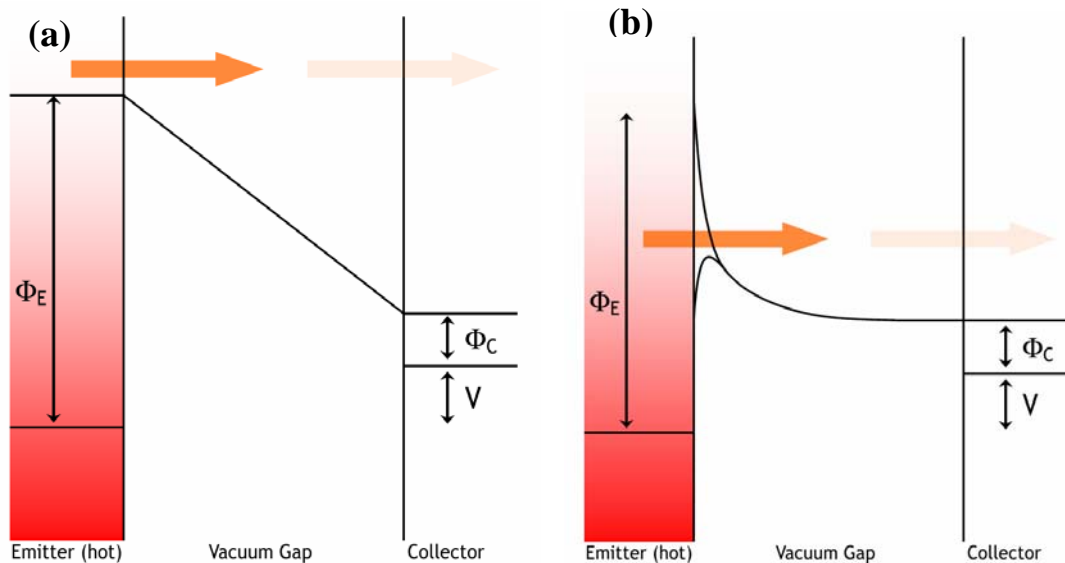

Fig. 9 Motive diagrams for thermionic energy conversion devices where a) represents a system that employs a flat surface emitter and collector, and b) represents a system with an emitter that has field enhancing structures on the surface. In both diagrams, Φ_E and Φ_C represent the work function of the emitter and collector respectively, and V represents the electric potential that develops due to the thermionic emission. The line in the vacuum gap represents the electric potential, and in b) the lower line represents the potential which includes Schottky lowering due to the image charge effect.

As indicated in the schematic, the barrier to emission is the work function of the emitter material; an electric potential V will develop at the cooler collector which can provide power to the electrical circuit. The advantage of this approach is that the vacuum blocks thermal transport by phonons (although radiative losses must be considered), and the barrier effectively selects hot electrons which leads to a high conversion efficiency. Thus conversion efficiencies greater than 20% can be achieved. The disadvantages are that since the work functions of most materials are greater than 3 eV, emitter temperatures greater than 1000ºC are required to achieve significant energy densities greater than 1W/cm^2. In addition, space charge effects cannot typically be neglected and the overall conversion efficiency may be substantially reduced.

Thus, the two primary goals of the research have been to explore new materials that would exhibit low work functions to enable operation at less than 1000ºC, and to explore approaches to minimize the space charge effects. Wide band gap semiconductors and nanostructured materials exhibit unique properties which can enable these approaches.

The wide band gap semiconductors of diamond and $Al_xGa_{1-x}N$ alloys have been shown to exhibit a small or negative electron affinity. This means that electrons excited into the conduction band may be emitted into a vacuum with little or no barrier. Thus n-type doping of the materials would provide electrons in the conduction band for efficient thermionic emission.

The approach for preparing an n-type diamond has been to employ nitrogen doping. N is known to be a relatively deep donor with a level at 1.7 eV below the conduction band minimum. However, simple calculations indicate that at temperatures of 500-600C, the Fermi energy would reside about 1.5 eV below the conduction band minimum resulting in an effective work function of 1.5 eV. Band bending effects would increase this value.

Research results on N-doped diamond thin films have indeed substantiated this prediction. A thermionic emission has been imaged using an electron emission microscope, and current versus temperature measurements have been analyzed, which indicated a work function of less than 2 eV. [34,35]

The thermionic emission current density versus temperature is typically analyzed with the Richardson equation. However, it is often difficult to separate effects due to a variation in the work function of the material and the Richardson constant, which is the prefactor term. Recent results have shown that it is possible to accurately determine the work function of the material by analyzing the spectrum of the thermionic emission. The lower energy cutoff represents the effective work function of the surface. The results for an N-doped diamond have indeed substantiated the analysis and established that the material does display an effective work function less than 2 eV.

The results for the AlGaN materials have been l worse than predicted. While high quality epitaxial growth and n-type doping have been achieved with both N-face and Al(Ga)-face orientations [36,37,38], the films displayed a work function significantly greater than 2.3 eV. This effect was attributed to upward band bending at the surface of the films. [36] While the states responsible for the band bending have not been identified, it seems likely that oxygen or other surface structures could cause the observed effects. We that further research into the surface preparation of the nitride materials could lead to lower work function surfaces, which could be appropriate for either emitter or collector applications in a vacuum TEC.

A single crystal diamond exhibits the highest thermal conductivity of any material and is optically transparent from the IR to the UV. These characteristics are important for a collector material. While obtaining single crystal diamond surfaces would be too costly for this type of an application, the development of approaches to grow highly oriented diamond (HOD) films could substantially impact these applications. [39] The HOD films exhibit thermal conductivity that approaches that of single crystal diamond. Finding approaches to dope the material to obtain significant n-type conductivity would be an important breakthrough.

The approach to mitigate the effects due to space charge involves employing a surface with field enhancing structures. The field enhancing structures include coated tips and nanostructured surfaces such as carbon nanotubes and nanocrystalline diamonds. As shown in Figure 9b, in the region of the tips there is a significant enhancement of the field, which leads to two important effects. [40] The first effect is Schottky barrier lowering due to the image charge, and the second is that the emitted electrons quickly reach their maximum energy, and the transit time across the cell is considerably slower than the flat surface. The first effect lowers the work function while the second effect reduces the space charge near the surface of the emitter. The first effect has been carefully modeled [40] using a finite element approach and specific dimensions corresponding to tip samples which were prepared and studied. [41]

The thermionic emission from nanocrystaline diamond coated tips, [41] carbon nanotubes [42] and nanocrystalline diamonds [43] have been measured. In all three cases, the field enhancing structures appear to result in significantly enhanced emissions when compared to similar flat surfaces without field enhancements.

In summary, the development of a vacuum TEC devices based on wide band gap materials and nanostructured materials holds significant potential for efficient energy conversion. Doped diamond has shown effective work functions of less than 2 eV, and nanostructured surfaces have indicated that field enhancing structures can lead to enhanced thermionic emission at very low applied fields. The goals ahead include improved materials for both emitters and collectors, and the development of a model to predict the performance of vacuum TEC cells with field enhancing structures.

SUMMARY
We are investigating new approaches for direct thermal to electric energy conversion, which have distinct advantages over the present state of the art: 1) improved thermoelectric/thermionic figure-of-merit (effective ZT) by both lowering the lattice thermal conductivity and increasing the thermoelectric power factor, 2) investigation of new metal/semiconductor compounds based on ErAs/InGaAs and TiN/GaN for thermoelectric applications, 3) lower temperature and highly efficient thermionic vacuum emitter-collector systems based on nanostructured diamond and nitrides, 4) integrated optimization of electrical, thermal and thermoelectric properties, 5) use of integrated circuit fabrication techniques for a scalable solution in the W-MW energy range 6) light weight and silent thin film devices.

ACKNOWLEDGEMENT

REFERENCES:

[1] D. Vashaee, A. Shakouri, "Improved Thermoelectric Power Factor in Metal-Based Superlattices" Physical Review Letter, Vol.92, no. 10, pp. 106103-1, 2004.

[2] A. Shakouri, "Thermoelectric, thermionic and thermophotovoltaic energy conversion" International Conference on Thermoelectrics, Clemson, NC, , pp. 492-497, 2005.

[3] Shakouri, A. and J.E. Bowers, "Heterostructure Integrated Thermionic Coolers," Applied Physics Letters, 71, pp. 1234-1236, 1997.

[4] Mahan GD, Woods LM. "Multilayer thermionic refrigeration," Physical Review Letters, vol.80, no.18, 4 pp.4016-19, May 1998.

[5] G.D. Mahan, and C.B. Vining, J. Appl. Phys. 86, 6852 (1999); R.J. Radtke, H. Ehrenreich, and C.H. Grein, J. Applied Physics 86, 3195 (1999).

[6] Ali Shakouri, Chris Labounty, Patrick Abraham, Joachim Piprek, and John E. Bowers, "Enhanced thermionic emission cooling in high barrier superlattice heterostructures", Material Research Society Symposium Proceedings, Vol. 545, pp.449-458, December 1998.

[7] D. Vashaee, A. Shakouri, Conservation of lateral momentum in heterostructure integrated thermionic coolers. Thermoelectric Materials 2001 - Research and Applications. Symposium (Materials Research Society Symposium Proceedings Vol.691). Mater. Res. Soc., pp.131-45. Warrendale, PA, USA, 2001.

[8] T.E. Humphrey and H. Linke, "Power Optimisation of Thermionic Devices" J. Phys. D. 38 2051 (2005).

[9] D. Vashaee, A. Shakouri. Electronic and thermoelectric transport in semiconductor and metallic superlattices. Journal of Applied Physics, vol.95, no.3, pp.1233-45, 2004.

[10] Singh R, Vashaee D, Yan Zhang, Negassi M, Shakouri A, Okuno Y, Gehong Zeng, LaBounty C, Bowers J. Experimental characterization and modeling of InP-based microcoolers. Thermoelectric Materials 2003 - Research and Applications Symposium (Mater. Res. Soc. Symposium Proceedings Vol.793). Mater. Res. Soc. 2004, pp.447-53. Warrendale, PA, USA.

[11] Daryoosh Vashaee, Yan Zhang, Gehong Zeng, Yi-Jen Chiu, and Ali Shakouri. Cross-Plane Seebeck Coefficient Anomaly in a High Barrier Superlattice with Miniband Formation. [Conference Paper] *Proceedings of the International Conference on Thermoelectics. Adelaide, Australia, July 2004*

[12] Zhixi Bian, and Ali Shakouri, "Enhanced Solid-state Thermionic Emission in Non-planar Heterostructures," to be published in Appl. Phys. Lett. 2006.

[13] T. E. Humphrey and A. Shakouri, "Transport formalism for multibarrier thermionic devices," Material Research Society Fall Meeting, Boston, MA, F7.3; manuscript under preparation.

[14] Kim, W., Singer, S., Majumdar, A., Zide, J., Gossard, A., and Shakouri, A., 2005, "Role of nanostructures in reducing thermal conductivity below alloy limit in crystalline solids," The 24th International Conference on Thermoelectrics, pp. 9-12.

[15] J. M. Zide, D. O. Klenov, S. Stemmer, A. C. Gossard, G. Zeng, J. E. Bowers, D. Vashaee and A. Shakouri, "Thermoelectric power factor in semiconductors with buried epitaxial semimetallic nanoparticles", Applied Physics Letters , 87 , pp.112102-1-3, September, 2005.

[16] Kim, W., Reddy, P., Majumdar, A., Zide, J., Gossard, A., D, O Klenov, S Stemmer, Zeng, G., Bowers, J., and Shakouri, A., 2004, "Beating the alloy limit of thermal conductivity in crystalline material," submitted to Physical Review Letters, 2005.

[17] Gehong Zeng, John E. Bowers, Joshua M. Zide, Yan Zhang and Ali Shakouri, Woochul Kim, Suzanne Singer, Arun Majumdar, Cross-plane Seebeck coefficient of ErAs:InGaAs/InGaAlAs superlattice, submitted to Applied Physics Letters 2005.

[18] J. M. Zide, D. Vashaee, G. Zeng, J. E. Bowers, A. Shakouri, A. C. Gossard, Demonstration of electron filtering to increase the Seebeck coefficient in ErAs:InGaAs/InGaAlAs superlattices, submitted to Physical Review B, 2005.

[19] A. Madan, I. W. Kim, S. C. Cheng, P. Yashar, V. P. Dravid, S. A. Barnett, Phy. Rev. Letters 78(9), 1743 (1997).

[20] M. Abu-Jafar, A. I. Al-Sharif and A. Qteish, Solid State Communications, 116, 389-393 (2000).

[21] V. Rawat and T. Sands TiN/GaN Metal/Semiconductor Multilayer Nanocomposites Grown by Reactive Pulsed Laser Deposition, MRS Proc. Vol 872, pp. J21.4.1-6 (2005).

[22] K.J. Russell, Ian Appelbaum, V. Narayanmurti, M.P. Hanson, and A.C. Gossard, Transverse momentum nonconservation at the ErAs/GaAs interface, Phys. Rev. B 71, 121311(R) (2005).

[23] Narayanamurti V, Kozhevnikov M. "BEEM imaging and spectroscopy of buried structures in semiconductors," Physics Reports, vol.349, no.6, pp.447-514, 2001.

[24] Reddy CV, Narayanamurti V, Ryou JH, Dupuis RD. "Current transport in InP/In/sub 0.5/(Al/sub 0.6/Ga/sub 0.4/)/sub 0.5/P self-assembled quantum dot heterostructures using ballistic electron emission microscopy/spectroscopy," Applied Physics Letters, vol.80, no.10, pp.1770-2, 2002.

[25] Yan Zhang, Vashaee D, Singh R, Shakouri A, Gehong Zeng, Yi-Jen Chiu. Influence of doping concentration and ambient temperature on the cross-plane Seebeck coefficient of InGaAs/InAlAs superlattices. [Conference Paper] Thermoelectric Materials 2003 - Research and Applications Symposium (Mater. Res. Soc. Symposium Proceedings Vol.793). Mater. Res. Soc. 2004, pp.59-65. Warrendale, PA, USA

[26] B. Yang, J. L. Liu, and K.L. Wang, and G. Chen "Simultaneous Measurements of Seebeck Coefficient and Thermal Conductivity Across Superlattice," Applied Physics Letters, Vol. 80, pp. 1758-1760, 2002.

[27] Gehong Zeng, John Bowers, Yan Zhang, Ali Shakouri, Josh Zide, Authur Gossard, Woolchul Kim, Arun Majumdar, "ErAs/InGaAs superlattice Seebeck coefficient", Proceedings of the 24 th International conference on Thermoelectrics , Clemson, SC; pp. 485-488, June, 2005.

[28] R. Venkatasubramanian, E. Siivola, T. Colpitts, and B. O'Quinn, Nature 413, 597-602, 2001

[29] Rajeev Singh, Zhixi Bian, Gehong Zeng, Joshua Zide, James Christofferson, Hsu-Feng Chou, Art Gossard, John Bowers, and Ali Shakouri, "Transient Harman Measurement of the Cross-plane ZT of InGaAs/InGaAlAs Superlattices with Embedded ErAs Nanoparticles" Proceedings of MRS Fall Meeting , Boston, November 2005.

[30] Zhixi Bian, Yan Zhang, Holger Schmidt, Ali Shakouri, [Conference Paper] Thin film ZT characterization using transient Harman technique, Proceedings of International Conference on Thermoelectronics, 2005.

[31] P. M. Mayer and R. J. Ram, 'Thin-film Thermoelectric Generator Element Characterization,' Proceedings of the 24th International Conference on Thermoelectrics, Clemson, S.C. pp. 265-8 (2005)

[32] P. M. Mayer, et al. manuscript submitted to Applied Physics Letters 2006.

[33] Gehong Zeng, John E. Bowers, Joshua M. Zide, Arthur C. Gossard, Woochul Kim, Suzanne Singer, Arun Majumdar, Rajeev Singh, Zhixi Bian, Yan Zhang and Ali Shakouri, ErAs:InGaAs/InGaAlAs superlattice thin film power generator array, submitted to APL Sept 2005.

[34] F. A. M. Koeck, J. M. Garguilo and R. J. Nemanich, "On the thermionic emission from nitrogen doped diamond films with respect to energy conversion," Diamond Relat. Mater. 13, 2052 (2004).

[35] F. A. M. Koeck, J. M. Garguilo and R. J. Nemanich, "Emission characterization from nitrogen-doped diamond with respect to energy conversion," Diamond Relat. Mater. 15, in press (2006).

[36] W. J. Mecouch, B. P. Wagner, Z. J. Reitmeier, and R. F. Davis, C. Pandarinath, B. J. Rodriguez, and R. J. Nemanich, "Preparation and characterization of atomically clean, stoichiometric surfaces of AlN(0001)," J. Vac. Sci. Technol. A 23, 72 (2005).

[37] R. Collazo, S. Mita, R. Schlesser and Z. Sitar, "Polarity control of Nitride thin films grown by metalorganic vapor phase epitaxy," Phys. Stat. Sol. (c) 2, No. 7, 2117-2120 (2005).

[38] S. Mita, R. Collazo, R. Schlesser and Z. Sitar, "Polarity control of GaN Films Grown by Metal Organic Chemical Vapor Deposition on (0001) Sapphire Substrates," Mater. Res. Soc. Symp. Proc. Vol. 831, E3.20.1 (2005).

[39] S. D. Wolter, D. Borca-Tasciuc, G. Chen, J. T. Prater, Z. Sitar, "Processing and thermal properties of highly oriented diamond thin films," Thin Solid Films 469-70, 105-111 (2004).

[40] J.R. Smith, R.J. Nemanich, G.L. Bilbro, "The effect of Schottky barrier lowering and nonplanar emitter geometry on the performance of a thermionic energy converter," Diamond Relat. Mater. 15, in press (2006).

[41] J. M. Garguilo, F. A. M. Koeck and R. J. Nemanich, X. C. Xiao, J. A. Carlisle and O. Auciello, "Thermionic Field Emission from Nanocrystalline Diamond Coated Silicon Tip Arrays," Phys. Rev. B 72, 165404 (2005).

[42] Y.Y. Wang, S. Gupta, J.M. Garguilo, R.J. Nemanich, "Imaging temperature-dependent field emission from carbon nanotube films: Single versus multiwalled," Appl. Phys. Lett. 86, 063109 (2005).

[43] F.A.M. Kock, J.M. Garguilo, R.J. Nemanich, "Field enhanced thermionic electron emission from sulfur doped nanocrystalline diamond films," Diamond Relat. Mater. 14, 704 (2005).